

RESEARCH ARTICLE

Performance analysis of power conditioning and distribution module for microsatellite applications

M. Bensaada , S. Della Krachai, F. Metehri, KDE. Kerrouche, MA. Mebrek, M. Beldjehem and F. Arezki

Centre of Satellite Development, Algerian Space Agency, Oran, Algeria

Corresponding author: M. Bensaada; Email: m.bensaada@yahoo.fr

Received: 24 August 2023; **Revised:** 21 March 2024; **Accepted:** 17 April 2024

Keywords: Spacecraft; Conditioning and distribution module; Switching; Overcurrent protection; Undervoltage

Abstract

Algeria's micro-satellite, Alsat-1b, was successfully launched into a 680 km low Earth orbit onboard a PSLV-C35 rocket from Sriharikota, South India, on September 26, 2016. The spacecraft was conceived, built and launched as part of an 18-month technology transfer programme between Algeria's Algerian Space Agency (ASAL) and the United Kingdom's Surrey Satellite Technology Limited (SSTL). This document details the Power Conditioning and Distribution Module's (PCM-PDM) design and performance in orbit, critical component of a satellite electrical power system, responsible for converting, regulating and distributing power to various subsystems and payloads. The PCM-PDM developed and produced by SSTL was subjected to rigorous testing simulating harsh space conditions to assess its performance. The results of this comprehensive analysis indicate that the module can effectively withstand extreme environmental factors and function optimally in challenging settings. The analysis focused on the PCM-PDM's ability to provide reliable and efficient power conditioning and distribution to the satellite, including its load management capabilities, overcurrent protection, protection against undervoltage and critical mode operations. The results of the performance analysis showed that the PCM-PDM met the required specifications and demonstrated reliable and efficient operation in different modes of the satellite's mission. The study highlights the importance of careful design and rigorous testing of the PCM-PDM to ensure the reliable and efficient operation of the satellite and its payloads.

Nomenclature

EoC	end of charge
$f_{cut-off}$	filter cut-off frequency
V_{ref}	voltage reference
$V_{shutdown}$	activation voltage
$V_{reactivation}$	reactivation voltage

1.0 Introduction

The Alsat-1B satellite, built on the SSTL-100 platform, is in a 700 km sun-synchronous orbit and weighs about 140.25 kg. The orbit period is 98.77 minutes, with around 64 minutes (or two-thirds of the orbit) spent in sunlight, and it orbits the Earth 15 times per day. The satellite is outfitted with a passive optical payload for remote sensing purposes. The satellite's nominal operating lifetime is 5 years, during which time the battery must maintain the whole satellite power requirements.

The spacecraft electrical power system (EPS) is responsible for generating, storing, conditioning, controlling and distributing power within a specified voltage range to all bus and payload equipment.

The power conditioning and distribution module (PCM-PDM) is a crucial subsystem in the EPS of a satellite. It is responsible for controlling and distributing power throughout the satellite, ensuring that all electronic devices and subsystems receive a regulated and conditioned source of electrical power. Overall, the PCM-PDM is a critical component of a satellite's electrical power system, responsible for ensuring the proper functioning and reliability of the satellite by regulating and distributing power to all electronic devices and subsystems [1].

The main function of the PCM is to regulate the power received from the solar panels or battery and ensure that it meets the required voltage and current specifications for the various loads on the satellite. The PCM also protects the satellite and its components from voltage spikes, surges and other electrical anomalies. In fact, the PCM is responsible for regulating the voltage and current of the power received from the solar panels or battery, protecting the satellite and its components from voltage spikes and surges, and managing the state of charge of the battery. Additionally, the PCM is responsible for managing the state of charge of the battery and ensuring that it is properly charged and maintained. This is important to ensure the long-term health and reliability of the battery, as well as to provide power to the satellite during periods of eclipse or low solar illumination [2]. The PCM also serves as a key component in the distribution of power throughout the satellite, providing a regulated and conditioned source of power to the other subsystems, such as the payload, communication and propulsion systems [3].

The PDM component of the PCM-PDM is responsible for distributing power to the various loads and subsystems on the satellite, including the payload, communication and propulsion systems. This is achieved through the use of switches and fuses, which are designed to protect the power system from faults in the user equipment, while also allowing for control over the spacecraft loads.

In addition to its power distribution and regulation functions, the PCM-PDM may also include monitoring and telemetry capabilities, allowing it to transmit data on the current consumption and load on each node to the on-board computer (OBC) for monitoring and control purposes [3, 4]. Power distribution provides a means of control over the spacecraft loads by:

1. The voltage and current for the spacecraft supply and individual loads need to be monitored (via the telemetry system)
2. Spacecraft loads need to be switched on and off (via the telecommand system)
3. Power system and other subsystems must be protected in the event of a short-circuit failure or overload of one subsystem or payload
4. Power switches must be:
 - Reliable
 - Low insertion loss
 - Withstand overloads
 - Re-settable current foldback
5. Hard wired (dangerous – no protection)
6. Fuses (dangerous – likely to fail due to vibration, etc.)
7. Power switches (transistor based on FET or bipolar)
8. Current limiter (resistors or more complex circuits)

The single bus voltage distributed architecture is a widely used design for small and large satellite spacecraft. It involves the distribution of a single voltage across the different subsystems, which then perform further regulation or point-of-load regulation. Some large satellites may have multiple voltage buses, such as a high and low voltage bus, but within each subsystem, there is typically one bus voltage.

Power switches are highly versatile tools for power distribution. They serve two main purposes. First, the power switch allows for telecommand activation and deactivation of subsystems, providing flexibility

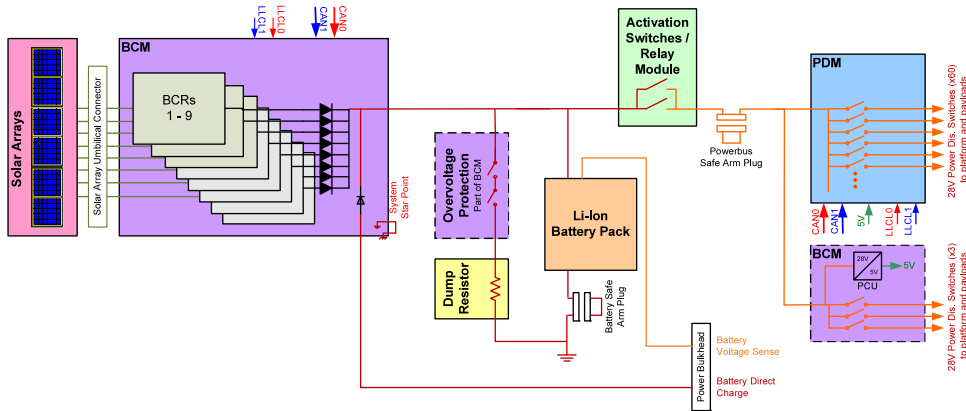


Figure 1. Alsat-1b power system architecture.

in power allocation and conserving resources when not required (power management). For example, turning off high-power transmitters during periods of high-power demand. Second, the power switch acts as a safeguard, functioning as an electronic fuse that cuts power to the subsystem if the current drawn exceeds a predetermined value, preventing damage to the system (protection). Switches are divided into two types: bipolar junction transistor (BJT) switches, including both positive and negative variants, and field effect transistor (FET) switches.

This paper focuses on detailing the design of the PCM-PDM for the microsatellite Alsat-1B. Serving as the backbone of the entire satellite system, the PCM-PDM plays a pivotal role in regulating power flow. The PCM-PDM receives unregulated 28V from the battery charge regulator (BCM) and subsequently distributes regulated 5V and unregulated 28V to the satellite’s loads. Within the PCM-PDM, functions such as current sensing, current limiting, switching and load protection are performed. The findings presented in this paper demonstrate that the PCM-PDM effectively executes all required operations while safeguarding against fault currents. The experimental results validate the system’s performance, showcasing its reliability and compliance with satellite requirements [5, 6].

2.0 Electrical power system architecture

Figure 1 depicts the block diagram of the Alsat-1b power subsystem. The subsystem is made up of four body-mounted solar panels with six solar array sections each, one BCM, one battery and one PCM-PDM. Each solar array portion is linked to one of the BCM’s battery charge regulators (BCRs). The main power bus, which is connected to the battery, is formed by combining all BCR outputs. During the day, each BCR manages the power from each solar array sector to correctly charge the battery based on the battery state of charge (SoC). In this setup, all available power from the solar panels is transferred to the main power bus while charging the battery and supplying the platform and payload modules.

If the battery is fully charged and reaches end of charge (EoC) voltage, the BCRs reduce their output power to supply only the power necessary for the spacecraft/satellite. When the power available during the sunshine time is insufficient, the battery discharges to support the difference, depending on the demand from the platform and payload modules. Because no power is generated by the solar panels during the eclipse, the battery is used to meet the system’s power requirements. There are mechanical activation switches between the main power bus and the power distribution side that cut power to the distribution side during launch and allow power flow soon after orbit injection. Following the activation of the switches, the main power bus is connected to the PCM-PDM and BCM for battery voltage distribution, regulated 5V generation and generated 5V distribution. These modules also protect the

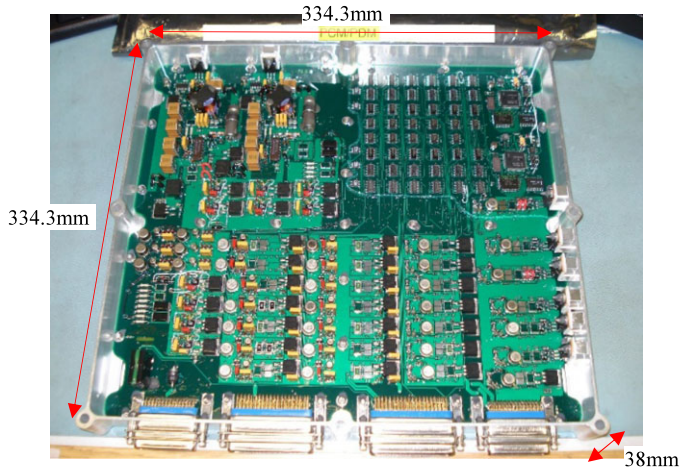


Figure 2. *Alsat-1b power distribution and conditioning module.*

power system main bus from a probable failure of one of the system's modules. For ground and launch side operations, the power subsystem architecture includes overvoltage protection circuitry, umbilical connections and external battery charge and voltage sensor connections [7, 8].

Figure 1 shows the Alsat-1b satellite power system architecture. The BCM converts the power required to charge a Li-ion battery and manages the main battery bus. The spacecraft loads are isolated from the battery during launch. Once separated from the launch vehicle, the activation switches automatically close. The unregulated primary battery bus powers the PCM-PDM's power conditioning units, which create a regulated 5V supply for the telemetry and telecommand (TTC) electronics. The PCM-PDM provides power to the platform and payloads via switches and fused wires.

3.0 Power conditioning and distribution module

The PCM-PDM, as illustrated in Fig. 2, is a combination of two modules: the PCM and the PDM. The total weight of the microtray and printed board assembly (PCA) is 1.838 kg.

The PCM composed of dual DC-DC flyback converters with a rating of 12.5 W, is responsible for generating the +5V bus in the power system. It has an input voltage range of 22 V to 34 V and provides power to the power subsystem CAN nodes and internal logic through the +5V bus. There are two redundant PCMs, PCMA and PCMB, that turn on simultaneously when the PCM-PDM is activated. PCMB's output is set slightly higher than PCMA, making it the prevailing voltage. The PCM also ensures the +5V output supply is protected against under-voltage and over-voltage conditions, shutting down the system if an overvoltage occurs on the 5V line. Additionally, it protects the battery from under-voltage by shutting down at a pre-set voltage level. The under-voltage protection level is normally set to 25V, and the PCM will restart when the voltage exceeds 27V [6].

The PDM section of the PCM/PDM features electronic power distribution switches and fuses to protect the power system from failures in sub-systems and payloads, as well as controlling the power distribution to maintain the system-level power budget. The PDM supplies the subsystems with both the unregulated battery voltage and the regulated +5V. The PCM-PDM serves as a buffer, transferring unregulated power from the battery/BCRs to the remainder of the spacecraft. The block diagram of the PCM-PDM is illustrated by the Fig. 3.

To prevent single point failures, redundant loads should be employed at the system level. All switches are commanded through a quad XOR gate, and redundant loads are assigned to switches on different XOR gates. Additionally, there are two battery voltage fused lines that are permanently used to power

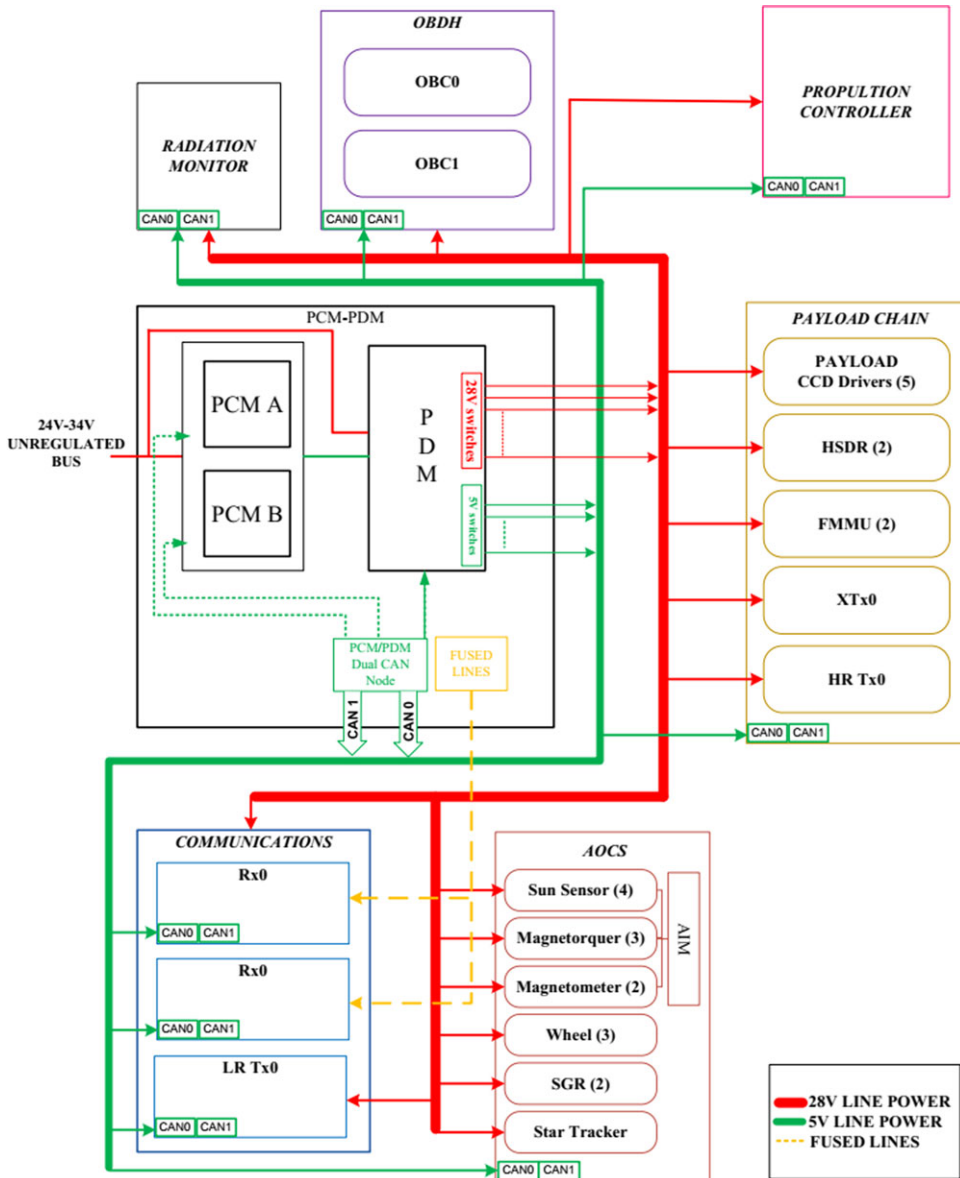


Figure 3. PCM/PDM block diagram.

the receivers. The fuses in these lines are paralleled for redundancy purposes. The PCM-PDM has dedicated, dual, hot redundant CAN nodes that are used to control the module through software and to transmit voltage, current, status and temperature telemetry data. Each CAN node in the PCM-PDM is connected to the CAN bus and a low-level command link (LLCL), which provides a direct connection to the receivers [8].

3.1 Power conditioning unit

The power conditioning module, depicted in Fig. 4, is a flyback type DC-DC converter that is responsible for generating the +5V bus within the power system. It operates using a current mode pulse width modulation (PWM) controller IC UC2842. The main power bus serves as the input for the PCM, which

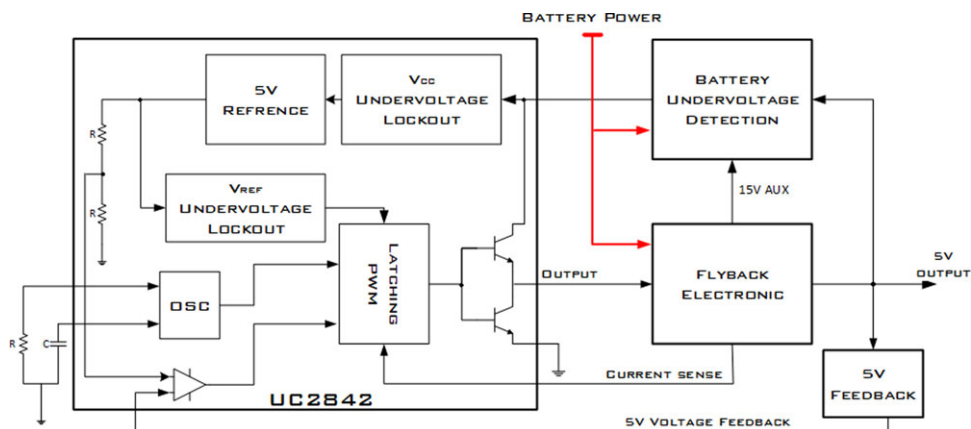


Figure 4. Alsat 1b power conditioning unit.

then steps it down to a regulated +5V bus that supplies power to the internal logic of the power subsystem and the CAN system power buses. There are two identical hot redundant PCMs (PCMA and PCMB), both of which activate when the PCM-PDM is powered. PCMB's output voltage has been set slightly higher than PCMA, making it the prevailing voltage with a nominal output of 5.25V (PCMB) or 5.15V (PCMA), depending on which PCM is active [9]. During worst-case transient conditions, the +5V bus will remain between 4.5V and 5.9V.

3.2 PCM voltage protection

The PCM provides under-voltage and over-voltage protection for its generated 5V output supply. An overvoltage condition on the 5V line will cause PCMB to trip off. Subsequent overvoltage conditions will cause the PCMs to switch over.

The PCM also provides under-voltage protection for the battery by shutting down at a pre-set voltage level which sets all power switches to the off position. The preset under-voltage protection level is nominally set to be 20V. A hysteresis loop starts the PCMs at a higher preset level nominally 22V when the battery recovers or is receiving power [10, 11].

3.3 Power distribution unit

The PDM is an indispensable component of a spacecraft's power system, acting as a vital shield against sub-system and payload failures. Its advanced design incorporates a combination of electronic circuit breakers and fuses that work in harmony to safeguard the power system, proactively preventing potential damage. The PDM additionally provides the capability to regulate power flow by selectively activating and deactivating systems, empowering effective management of the power budget. Acting as a crucial bridge between the unregulated battery voltage and the regulated +5V, the PDM ensures a smooth and stable power supply to the sub-systems. Moreover, it serves as a protective buffer between the unregulated power source from the battery and the rest of the spacecraft, assuring a constant and dependable power distribution throughout. In conclusion, the PDM is an essential and sophisticated element of the spacecraft's power system, providing reliable protection and precise control to ensure optimal spacecraft operation.

The task of the PDM is to deliver various voltages to the spacecraft/satellite; it may be turned on and off through telecommand. The switch is also an electronic fuse that automatically shuts off when the current drawn by the sub-system exceeds a pre-set value [2].

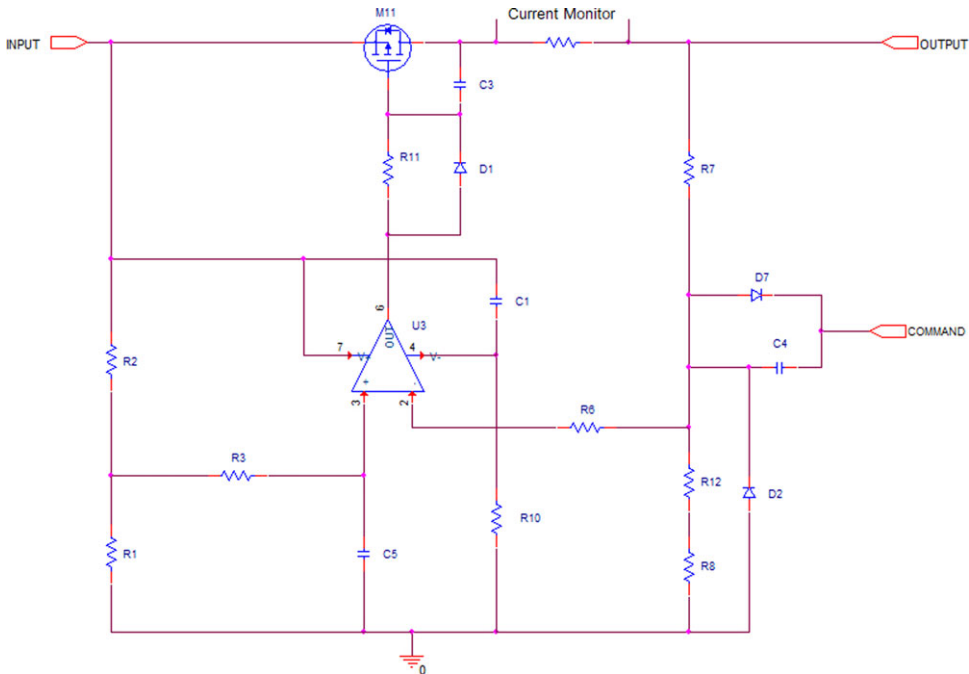


Figure 5. The FET switch.

3.4 5V switches

There are two distinct categories of 5V switches, each with a variable trip setting that can be adjusted at the time of switch allocation. These adjustable trip settings allow for greater flexibility and customisation, ensuring that the switch can meet the specific requirements of each individual application. This feature enables the switch to be tailored to the specific power and current needs, providing a high level of protection to the connected system. The ability to adjust the trip setting in this manner enhances the reliability and longevity of the switch, making it a valuable component in a wide range of electronic systems [2, 8].

- 10× FET switches rated to a maximum of 2A
- 6× BJT switches rated to a maximum of 500mA (not suitable for the Alast-1B mission due to their high sensitivity to temperature changes)

3.5 FET switch

Bipolar transistor switches are known for their inefficiency when handling larger currents. To address this issue, a new FET-based power switch has been developed, as depicted in Fig. 5. This switch operates similarly to the bipolar power switch, with the main difference being that the P channel FET is turned on (equivalent to zero volts) when the gate voltage is at a low level [5, 7]. On the other hand, when the gate voltage is equal to the source voltage, the FET is turned off.

When the output is low and the input is high, the switch is in the off state. The positive input of the comparator is maintained at approximately 3.5V by the voltage bridge divider circuit consisting of R1 and R2, making it higher than the negative input. As a result, the output stays high, keeping the FET turned off.

When the command line is at a high voltage, a 5V pulse is applied to capacitor C2, causing the negative input to become higher than the positive input. As a result, the comparator output goes low,

switching the FET on. During normal operation, the negative input is slightly above the positive input, resulting in the switch being in the on state. To turn the switch off, a low-going pulse is applied to the capacitor, causing the negative input to drop below the positive input, and the switch to turn off, similar to a bipolar switch.

To determine the trip current, the voltage drop across the FET is calculated. Since the internal resistance of the FET is relatively stable, as the current increases, the voltage drop across the FET increases linearly. This increase in voltage drop leads to a decrease in both the output voltage and the voltage at the negative input of the comparator. Consequently, when the negative input drops below the positive input, the switch is turned off [7].

The value of the select-on-test resistor R8 is adjusted to determine the trip current. By increasing the voltage drop across this resistor, the voltage on the negative input becomes higher than the positive input, resulting in an increase in the trip current. To avoid sudden changes in the input from tripping the switch, a low-pass filter is incorporated into the positive input of the comparator. This filter restricts the cut-off frequency, as defined in Equation (1).

$$f_{cut-off} = 1 / [2\pi \times ((R_1 R_2 / (R_1 + R_2) + R_3) \times C_3)] \quad (1)$$

3.6 Battery voltage switches

The power conditioning module and power distribution module are designed with three distinct versions of battery voltage switches, each of which is equipped with a configurable trip setting, providing greater versatility and adaptability [8, 12, 13].

- 14× foldback current latch switches rated to a maximum of 2.5A (low power).
- 8× timed current latch switches rated to a maximum of 5A (medium power).
- 6× timed current latch switches rated to a maximum of 7.5A (high power).

3.6.1 Foldback current latch switch

The circuit diagram of the foldback current latch switches (FCL) is depicted in Fig. 6. The switch is activated by providing a +5V signal to the command line. When the current exceeds the pre-set trip level, the switch will initiate current limiting. During this process, if the output voltage drops, the current limit will decrease to a low level in order to reduce FET heat generation. To restore the switch, the load must be reduced below the lower limit, and the switch must be turned off and then re-activated [14–16].

3.6.2 Timed current latch switch

The circuit, as depicted in Fig. 7, features a total of eight 5A timed current latch (TCL) switches and six 10A TCL switches, along with an additional six TCL switches rated at 7.5A. Activation of the switch is achieved by driving the command line high while simultaneously pulling current through R322. If the current surpasses the established trip threshold, the switch will limit the current flow for 4 milliseconds before locking off. To reset the switch, simply toggle it off and then on again [17–19].

3.7 Fused lines

3.7.1 Battery voltage supply

To keep critical equipment such as receivers running, there are two specific battery voltage lines with fuses that must remain continuously energised. In case of a backup, switches 27 and 28 can serve as additional fused lines. To guarantee dependability and long-term performance, each of these lines has two parallel 1A fuses, with one fuse also featuring a resistor to counteract the effects of aging.

3.7.2 PCM-PDM 5V CAN supply

The PCM-PDM utilises 5V fused lines to supply the necessary power to its internal CAN circuitry. For each CAN node, two 1A fuses are installed in parallel to ensure robust protection. Additionally, one of

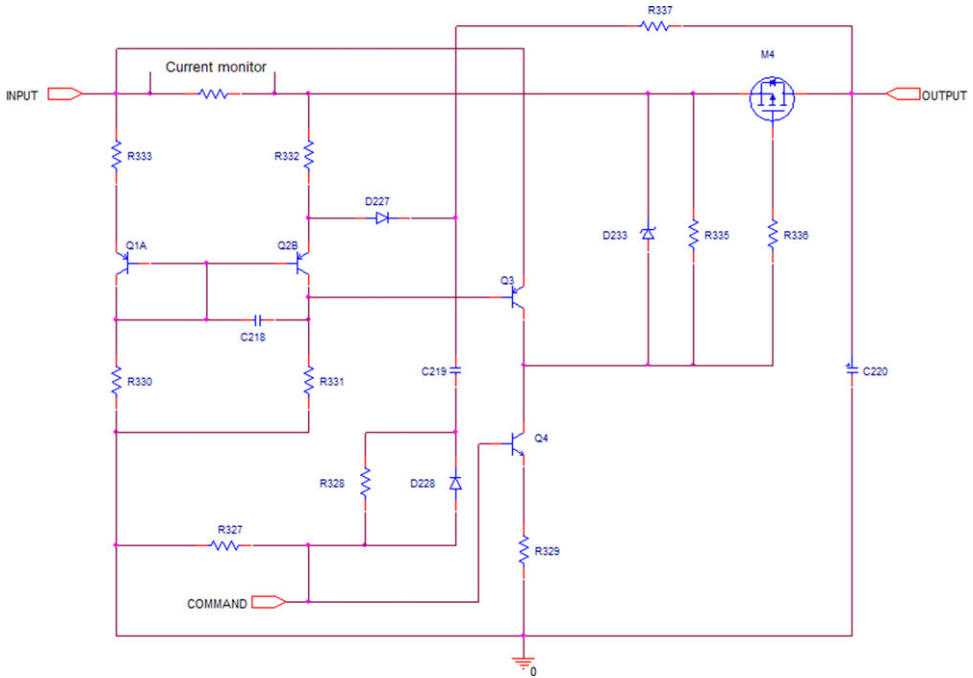


Figure 6. 28V foldback current latch switch.

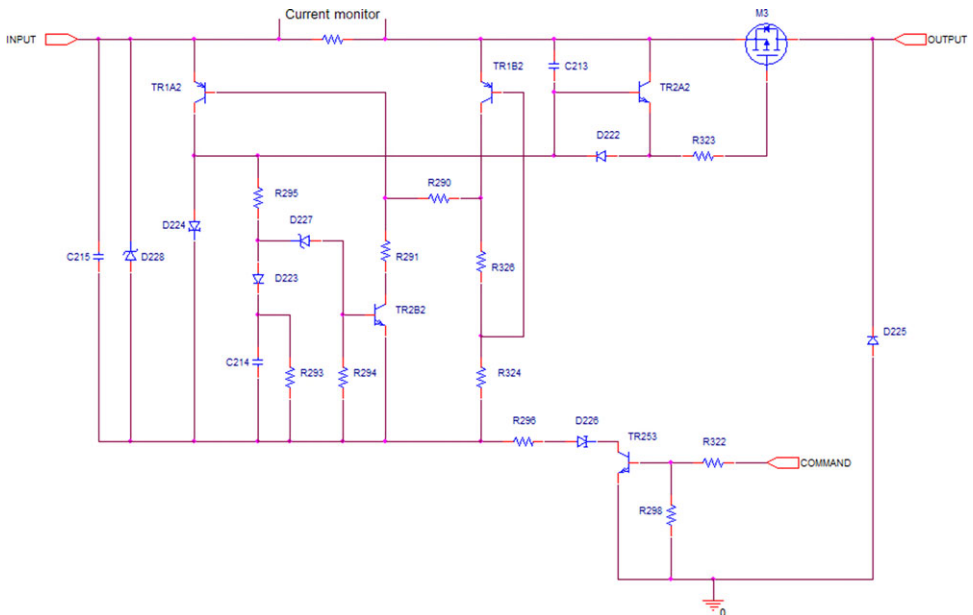


Figure 7. 28V timed current latch switch.

the fuses is connected in series with a resistor, which helps to mitigate the aging effect and prolong the longevity of the system.

3.7.3 BCM 5V CAN supply

The BCM gets its power for its CAN circuitry from the 5V fused lines provided by the PCM/PDM. To ensure robust protection, each CAN node is fitted with two 1A fuses arranged in parallel, with one of

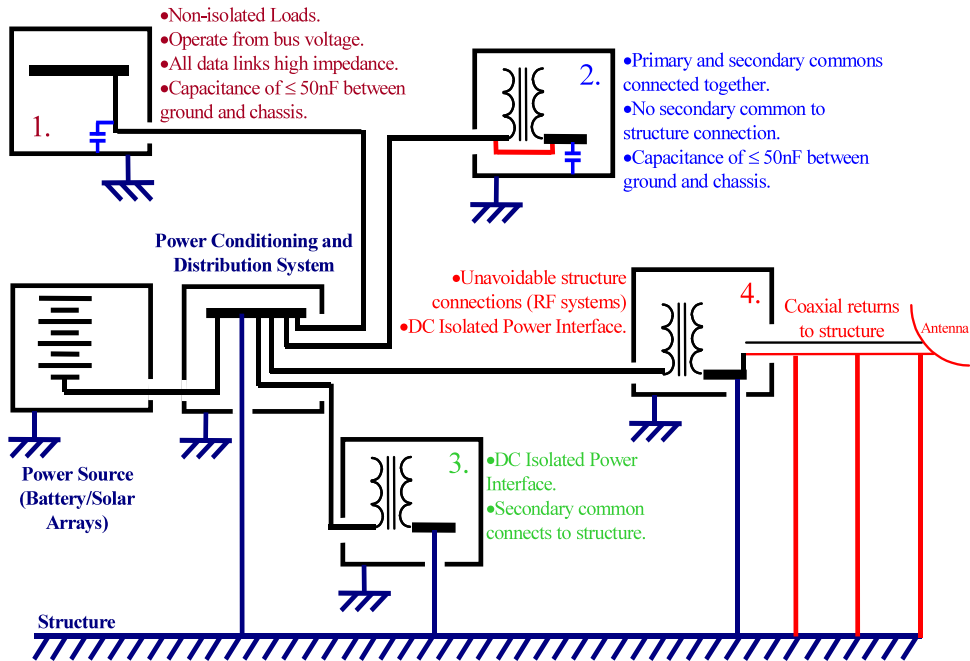


Figure 8. Grounding scheme [8].

the fuses further connected to a resistor to minimise the impact of aging. The BCM's own fused lines are supplied with power from these 5V fused lines. If a single power board is enough, one set of these fused lines can be removed and replaced with wire connections.

However, in cases where multiple power boards are deployed, such as when additional BCMs or switch boards are present, the 5V CAN supply must be connected in a circular configuration to connect all boards. In this scenario, the fuses on the PCM/PDM should not be used, as they are designed to accommodate only two CAN nodes. Instead, wire connections should be established, followed by the installation of the CAN fuses on each individual power board.

3.8 CAN bus circuitry

The PCM-PDM boasts two highly reliable and redundant CAN nodes for both software control and telemetry transmission. The telemetry data and commands are loaded onto the erasable programmable read-only memory (EPROM) chip through the firmware, which then seamlessly integrates with the CAN node circuit. In normal operations, the onboard computer manages the telemetry and instructions effectively. However, in the event of a failure of the onboard computer or malfunction of the CAN bus, the PCM-PDM provides a low-level command interface as a backup, allowing for direct transmission of commands through the receivers. This redundant design guarantees the stability and dependability of the module [8].

3.9 Grounding and isolation scheme

The objective of the SSTL power grounding and isolation technique is to eliminate DC ground loops and reduce AC disturbances among bus users. This is achieved by minimising the total main ripple currents that flow through shared return pathways and structures. The method has been successfully implemented on previous SSTL small spacecraft in low Earth orbit (LEO) and medium Earth orbit (MEO). The entire power system was designed with the assumption that the grounding policy outlined in Fig. 8 would be incorporated into the spacecraft design [20–22].

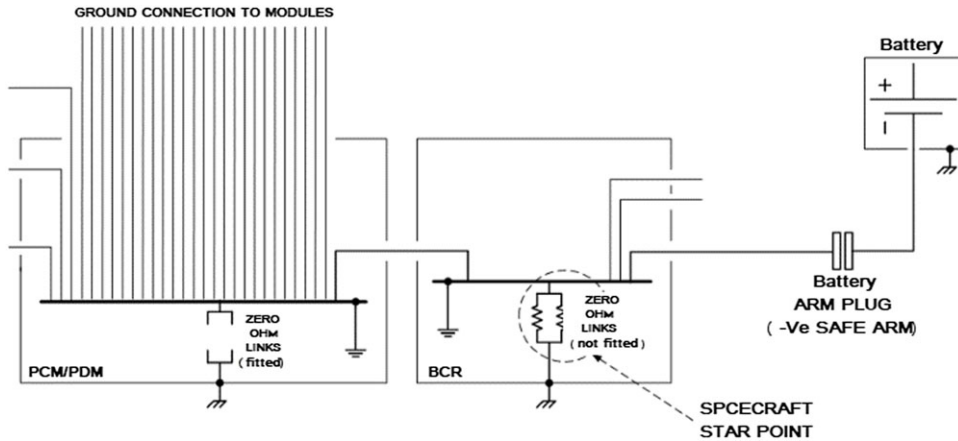


Figure 9. Power system grounding diagram.

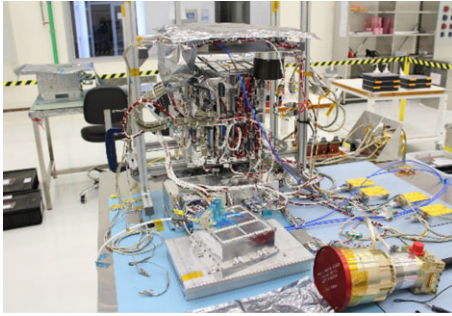
The power system is composed of two main electronic modules: the BCR and the PCM-PDM, along with the solar arrays and battery that complete the system. The spacecraft star point, which is a central location where the unit-level ground planes or return lines are electrically connected to the spacecraft structure, is situated within the BCR. Currently, the star point is housed in the BCM for grounding purposes. However, if needed, the star point can be relocated to the PCM/PDM to meet specific requirements [23].

The PCM-PDM is connected to the BCR ground plane by bypassing the local star point, as depicted in Fig. 9. The negative battery connection is also linked to the BCR through the battery arm plug (-Ve safe arm). The BCR and PCM-PDM provide switched lines to all other modules and equipment on the spacecraft, with the BCR supplying unregulated 28V switches and the PCM-PDM offering both unregulated 28V switches and 5V regulated switches. Each switched line is accompanied by a corresponding ground line, which grounds the module ground plane for non-isolated modules or the return line for isolated modules, depending on the chosen isolation scheme [8, 24].

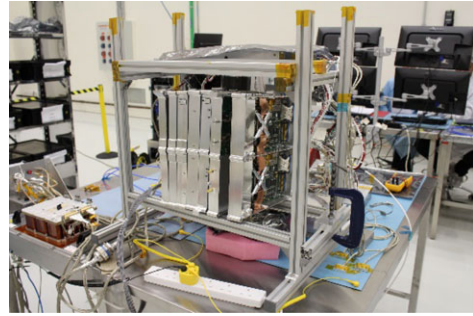
4.0 Module tests

The PCM-PDM test is a crucial step in ensuring the reliability and performance of the module. This test evaluates the module's ability to control and distribute power from the solar arrays and battery to the rest of the spacecraft. The test procedure typically involves a series of electrical and functional tests, including input/output voltage and current measurements, as well as testing of the protection circuits and fault management strategies. In addition, the performance of the module's telemetry system, which is responsible for transmitting data and commands, is also assessed. The PCM-PDM test is critical in verifying that the module meets the design specifications and requirements, and that it is ready for integration with the rest of the spacecraft subsystems. The tests performed are organised into the following categories:

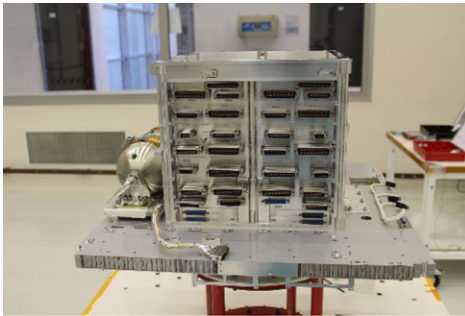
1. In order to eliminate infant mortalities before system level testing, it is imperative to subject all modules to a burn-in test to ensure they accumulate a total on-time exceeding 168 hours (equivalent to seven days). The burn-in test must be completed prior to the system thermal vacuum testing to guarantee reliable and optimal performance.
2. The first step in integrating the various sub-systems of the platform involves assembling them in a soft stack configuration. Each module undergoes individual testing in the laboratory before being integrated into the satellite structure for comprehensive testing. Modules and the battery



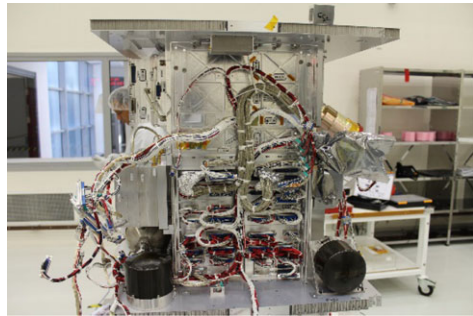
Front view



Back view

Figure 10. *Soft stack configuration and test.*

Central Stack



Hard Stack

Figure 11. *Hard stack configuration and test.*

are flexibly assembled on a table using the designed harness, forming what we refer to as a soft stack. This approach facilitates testing of the entire system. In the event of a subsystem anomaly, disassembly is unnecessary, mitigating any associated risks or accidents. This step aims to verify the interconnection of the modules and test their functionalities. This is made possible by the modularity of the SSTL platforms, which consist of several electronics boxes that are mounted together to create the core stack. To facilitate the integration process, module boxes are positioned on their sides within integration stands and secured using integration clamps. This straightforward approach minimises the effort required to remove individual units in case any issues arise during the integration process. Figure 10 illustrates of this approach to initial module integration. The aim of this initial module integration is to conduct initial checks on each of the individually tested modules to verify that each one fits and functions with the harness. Power, grounding and isolation is checked on each module, and harness power checks are performed prior to module connections to confirm voltage level and polarity. Once this has been completed, the module will be electrically connected; at this stage modules and flight harness connectors will use connector savers. The main advantage of this framework is that a module can be easily inserted and taken out if required, irrespective of its position in the stack. If the module works with the power system and telemetry can be obtained, then the module can be integrated regardless of whether certain other modules are present or not.

3. The last step in the platform assembly process involves the final platform hard stack procedure, this implies that all modules are assembled within the satellite structure to undergo rigorous environmental testing as shown in Fig. 11, which encompasses assembling the complete platform into its designated flight configuration. This includes ensuring that the platform fixings are tightened to their appropriate torque levels and that the flight harness is connected to modules

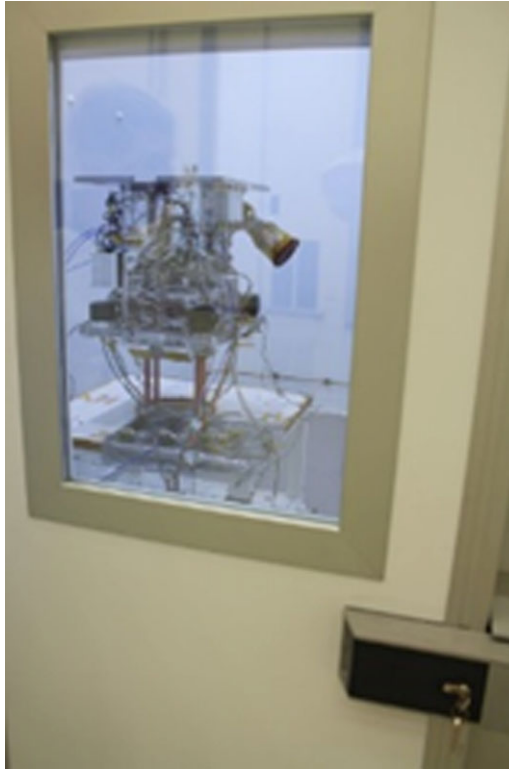


Figure 12. Alsat-1B in thermal cycle test chamber.

with the connector savers removed. Additionally, the propulsion subsystem is integrated into the spacecraft during this process. It is crucial to note that even in this fully assembled configuration, the spacecraft can be disassembled seamlessly if any issues arise during functional testing.

4. The objective of conducting platform ambient pressure thermal cycle tests is to evaluate the spacecraft's performance across a broad temperature range, typically ranging from -20°C to $+50^{\circ}\text{C}$. The test procedure includes at least one round of thermal cycles, consisting of three hot/cold cycles. The tests assess the power consumption levels, interfaces and overall functionality of the platform under various temperature conditions. Furthermore, the cold start of the platform is performed to assess the efficiency of battery charging and power regulation, as well as the RF system's bit error rate and TTC functions. The tests also involve evaluating the robustness of cross-strapped interfaces and redundant data bus (CAN bus). So, to verify the functionality of the platform's electrical interfaces in the flight configuration under varying temperatures, an ambient pressure thermal cycle campaign is conducted. Each module must undergo a minimum of one round of thermal cycling, which comprises three cycles of hot and cold temperatures. However, some modules may undergo more than one round of thermal cycling based on the schedule. This process as shown in Fig. 12, ensures the robustness of the platform's electrical interfaces, guaranteeing their stable operation under extreme conditions.
5. When significant hardware changes are made, the units are subjected to unit level qualification vibration tests to ensure their reliability (see Fig. 13). The unit is subjected to qualification loads that simulate the expected launch environment for the particular unit. Typically, the tests involve both random vibration and sine sweep. For generic hardware units, a more generalised spectrum is used to cover a wider range of launch environments. By conducting these tests, the unit's capability to withstand the harsh launch conditions is verified, ensuring that it operates safely and



Figure 13. *Alsat-1B vibration tests.*

effectively during the launch phase. obviously, a functionality test is carried out both prior to and subsequent to the vibration test. This is done to confirm that the unit is operating correctly and effectively, both before and after being exposed to the vibration test. This process helps to identify any issues or anomalies that may have arisen due to the vibration test, and ensure the unit's reliability and functionality under normal operating conditions. By conducting these tests, the unit's ability to perform its intended functions is verified (pre/post vibration module test), which is crucial to its successful operation. The satellite undergoes a comprehensive vibration qualification test campaign, encompassing modal, sine sweep and random vibration tests. Notably, the initial frequency of the satellite is 68 Hz, meeting the launcher's requirements. Furthermore, all modules and the satellite itself successfully endure random and sine sweep vibrations, with amplitudes ranging from 0 to 2000 Hz falling within the qualification envelope of each module. No damage was observed in the satellite structure throughout these tests.

6. The EMC test campaign as shown by Fig. 14 serves a critical purpose in verifying the spacecraft's compatibility with the launch vehicle, minimising the likelihood of incompatibilities that may lead to severe mission delays or the loss of a launch opportunity. Moreover, as a secondary objective, the campaign also validates the functionality of the spacecraft systems in their flight configuration, further reducing the risk of system malfunctions during launch and operation. By fulfilling both these objectives, the EMC test campaign plays an essential role in ensuring the success of the spacecraft launch and mission.

The full set of tests performed cover:

- Radiated emissions (launcher and range compatibility)
- Radiated susceptibility (launcher and range compatibility)
- Spacecraft self-susceptibility tests (under various predefined operational modes)
- Spacecraft antenna functional checks
- Payload compatibility
- Spacecraft wireless operation (end to end testing)

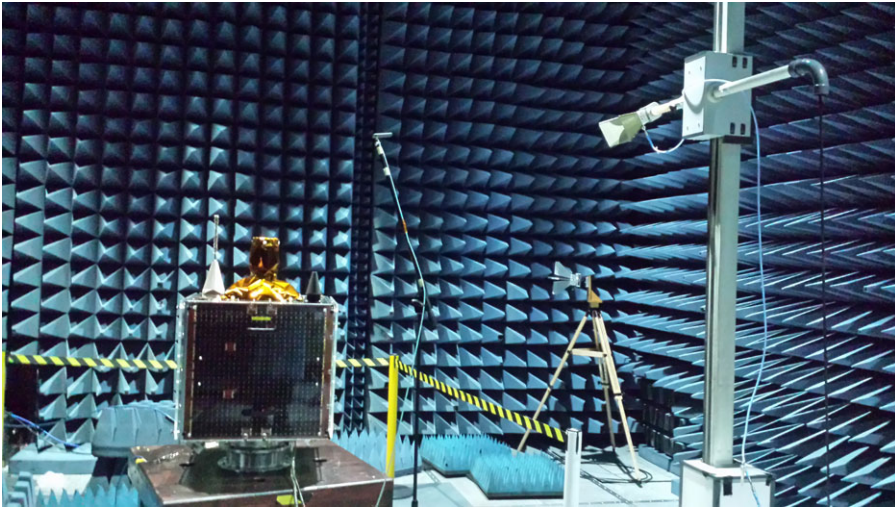


Figure 14. Alsat-1B in EMC test chamber.

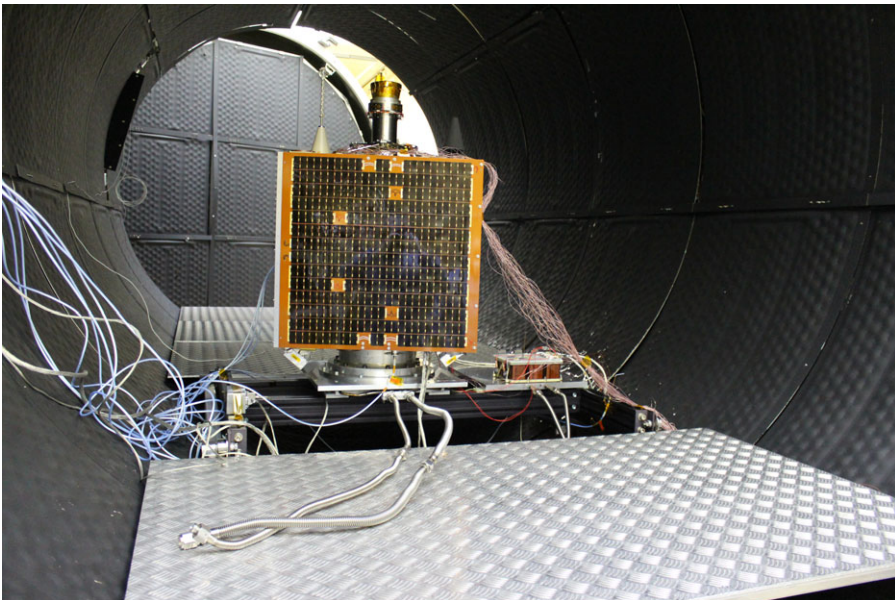


Figure 15. Alsat-1B in TVT test chamber.

7. The main aim of the thermal vacuum testing (TVT) test is not to replicate the space environment during different mission phases. Instead, its primary goal is to confirm the spacecraft's performance under high vacuum conditions and extreme temperatures, both hot and cold. To achieve this, a balance is maintained to subject the spacecraft to sufficient thermal stress to reveal any potential design or manufacturing weaknesses, while ensuring that flight hardware is not overstressed. In doing so, the testing indirectly validates the effectiveness of the spacecraft's thermal design (see Fig. 15) by verifying elements of the thermal model used in its construction. The test methodology involves cycling the shroud and base plate repeatedly between the required temperature extremes, as many times as possible within the test campaign's allotted time frame. Simultaneously, the electrical operation of every subsystem and payload is tested to ensure their

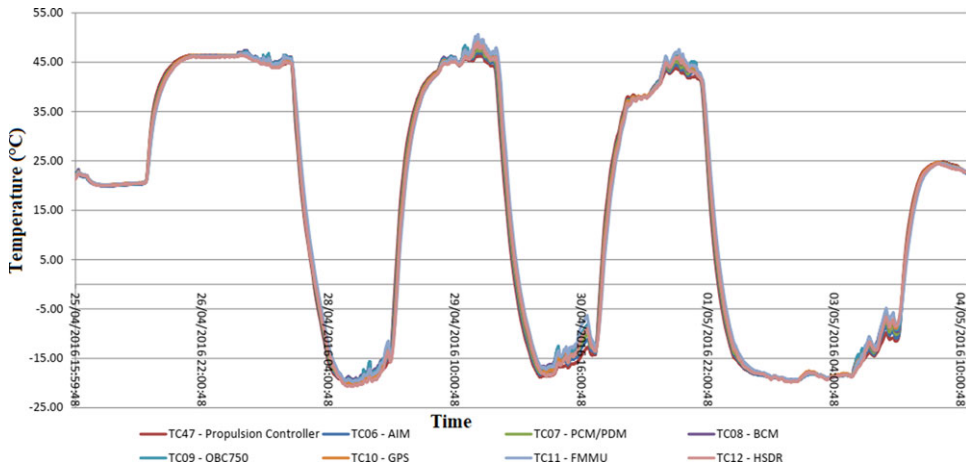


Figure 16. PCM-PDM temperature in TVT test chamber.

proper functioning. Specifically, the capability to switch on and off systems under both hot and cold temperature conditions must be validated.

8. The aim of the thermal cycle control is to allow each unit to be tested (see Fig. 16) at its desired temperature without allowing other units to go beyond their limits. In practice this is likely to mean that not all units will be tested at the full extremes of $+50^{\circ}\text{C}$ to -20°C , in this case the tests will be carried out at the widest temperature range possible and must be inside the boundary set by the operational predictions, However, it is crucial to note that the spacecraft battery should only be charged between 0°C and $+30^{\circ}\text{C}$, and this parameter must be strictly adhered to during the testing.
9. The checkout procedure at the launch site for the AlSat-1b spacecraft is crucial. Given the constraints of time, it becomes challenging to conduct comprehensive electrical tests for all the spacecraft hardware. Therefore, this step must be executed meticulously to ensure the spacecraft's readiness for launch. The purpose of this test procedure is to:
 - Visually confirm that spacecraft have not been damaged during transportation to the launch site.
 - Set up the electronic ground support equipment (EGSE) racks ready for launch site testing.
 - Perform battery checkout and storage recovery and charging of the flight battery.
 - Conduct baseline functional tests of spacecraft modules.
 - Conduct limited and payload interface testing.
 - Implement red tag/green tag item installation and removal and solar array functionality.
 - Perform propulsion system filling.

4.1 Grounding and isolation scheme

The PCM is the first component of the PCM-PDM that must be operational for the testing process to proceed. This is because the 5V line generated by the PCM is responsible for powering the electronics and logic used in the power system, making it essential for conducting further tests. The PCM has two redundant modules, A and B, with B set to a higher voltage level to take over in the event that both are activated. A block schematic of the PCM electronics is shown in Fig. 17.

The first stage of the testing procedure involves determining the switching frequency of the PCM. This step evaluates the operating frequency of each power conditioning module to confirm that it conforms

Table 1. PCM operating frequency and voltage reference

PCM	Expected Frequency (kHz)	Measured Frequency (kHz)	Expected V_{ref} (V)	Measured V_{ref} (V)	Bus Voltage (V)	Expected Current Consumption (mA)	Measured Current Consumption (mA)
A	100kHz	97	$5V \pm 0.05V$	4.98	5.153	< 45	34
B	$\pm 5kHz$	98		4.99	5.253		

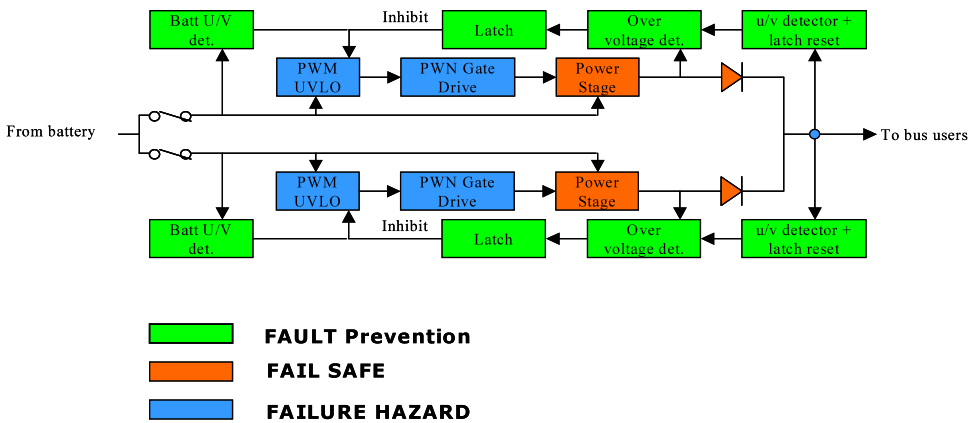


Figure 17. PCM electronics.

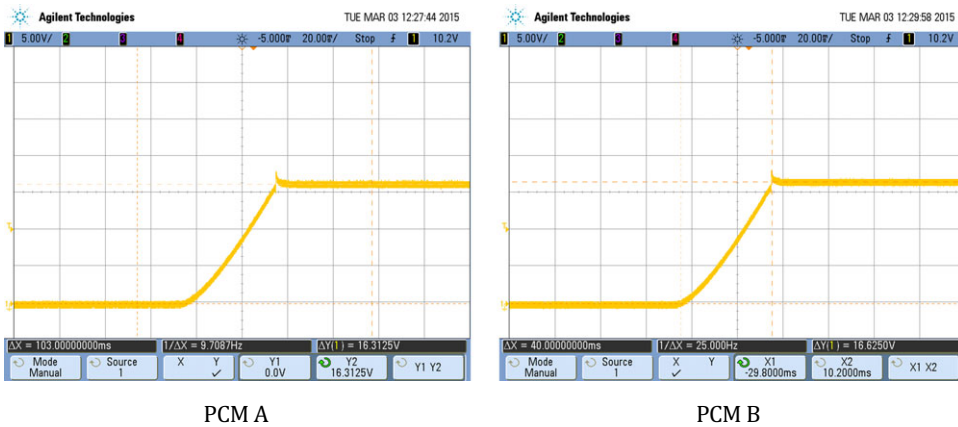


Figure 18. PCM Aux-winding waveform.

to the established standards, and examines the precision of the internal voltage reference in the pulse width modulation integrated circuit (PWM IC). The outcome of these assessments are documented and presented in a comprehensive manner in Table 1.

The PCMs begin operating once the supply voltage is applied to the PWM ICs (UC2842). A waveform is generated in the auxiliary winding of the PCM inductor, which is then rectified, producing a DC voltage of 16.1V for PCM A and 16.62V for PCM B (as depicted in Fig. 18). The higher voltage of PCM B allows it to supply power to the UC2842 after start-up.

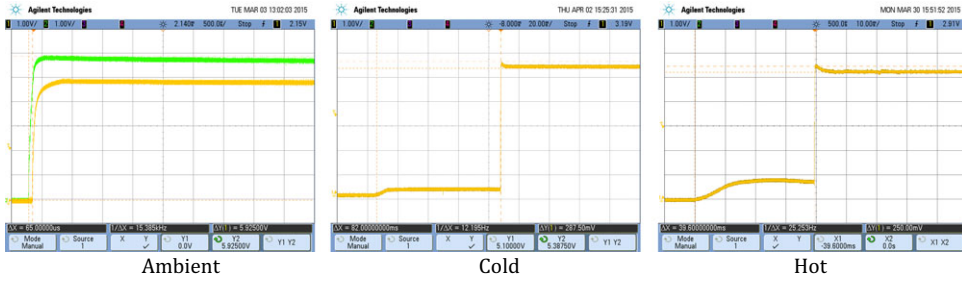


Figure 19. PCM start-up waveform for different temperature.

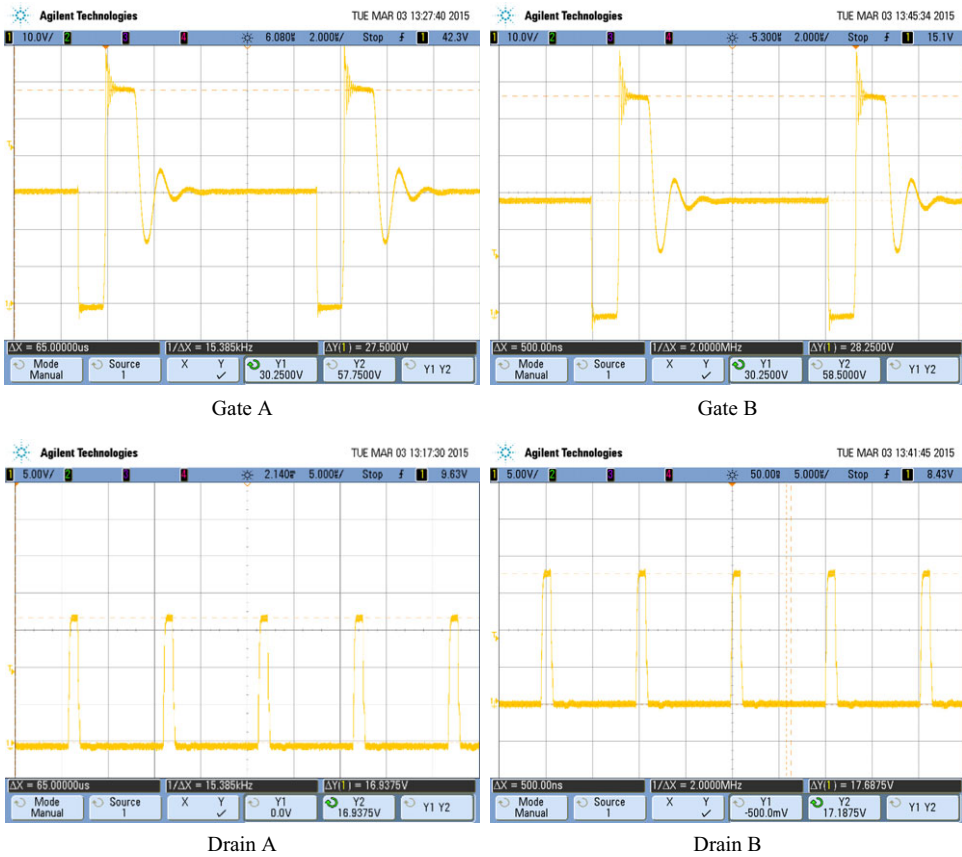


Figure 20. PCM gate and drain waveforms.

At the start-up of the PCM, an overshoot is observed on the 5V line. This overshoot can cause the PCM to shut down immediately after being turned on if it exceeds a certain limit. Figure 19 illustrates this phenomenon, where the peak voltage reached 5.925V and the time between PCM A and B turning on was approximately 65 μ s. It is important to ensure that the overshoot on the 5V line remains within acceptable limits to prevent the PCM from tripping off.

The traces of the flyback MosFET gate and drain are shown in Fig. 20. The peak gate voltage measured was 16.93V for PCM A and 17.18V for PCM B, which is within the acceptable range of 12–18V. The measured ripple voltage was approximately 15mV for PCM A and 16mV for PCM B, which is well below the acceptable limit of 100mV.

Table 2. PCM battery voltage shutdown/restart

Required Shutdown Voltage (V)		21.6
PCM	V_{Shutdown} (V)	$V_{\text{Reactivation}}$ (V)
Ambient	21.71	23.92
Hot	21.65	23.88
Cold	21.65	23.85

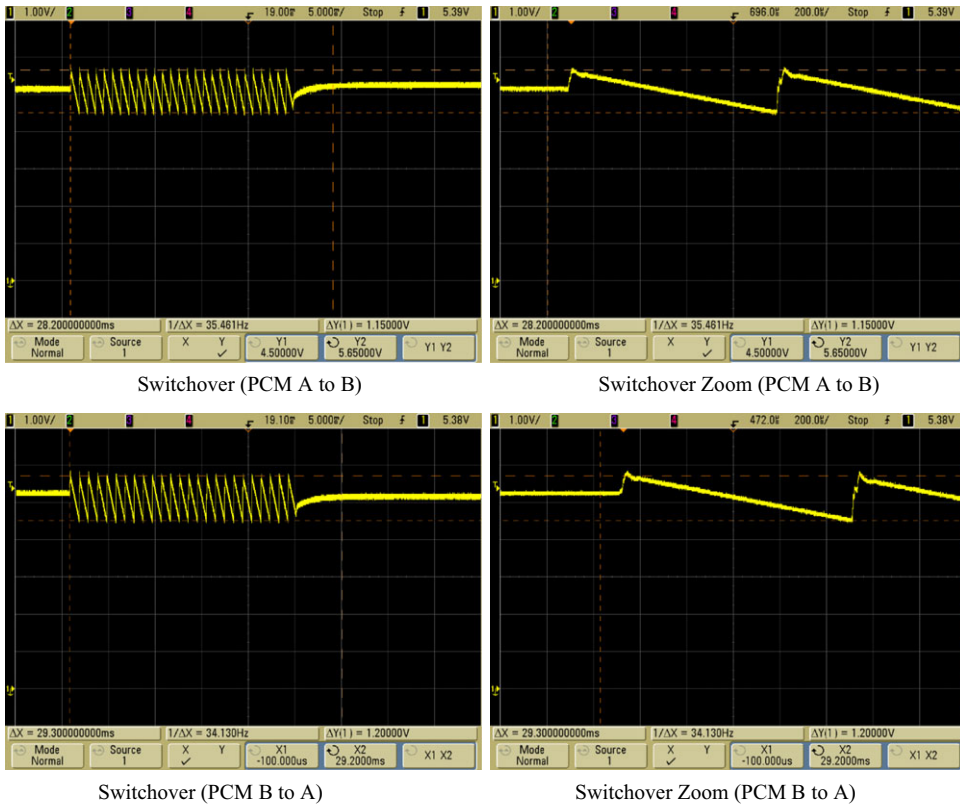


Figure 21. PCM switchover transient waveform.

The PCMs also feature an automated under-voltage cut-off function, which automatically turns off the PCM if the battery voltage drops below a predetermined level. This helps to ensure that the battery voltage does not fall to an unrecoverable level and prevent it from being subjected to excessive strain. The PCM’s reactivation voltage is approximately 2V higher than the shutdown voltage, which creates a hysteresis effect. This helps to prevent the PCM from rapidly switching between the on and off states and allows the battery to recharge. The test results of this function can be found in Table 2.

The PCMs are designed to function as hot redundant switchovers. The testing procedure involves simulating an over-voltage condition on each PCM output, which causes the affected PCM to turn off and triggers a switchover to the other PCM. The complete switchover waveform is depicted in Fig. 21, and a zoomed-in version of the waveform provides a closer look at the voltage levels during the initial transients.

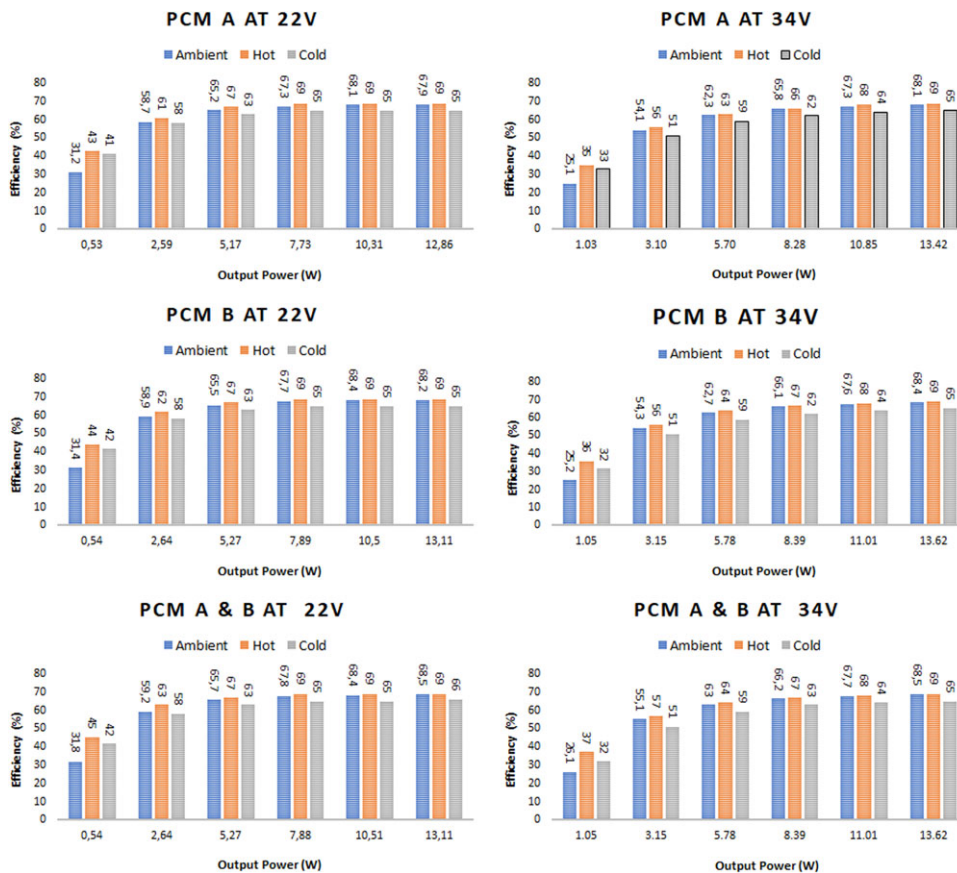


Figure 22. PCM efficiency at minimum and maximum voltage.

The PCMs have a maximum rated output current of 2.5A, and it is important to ensure that this limit is not exceeded. Testing should be performed at various input voltages of 22V (best case), 28V (nominal case) and 34V (worst case) for each PCM combination, including PCMA only, PCMB only and PCMA + B. The efficiency of the PCMs for each scenario is represented in Fig. 22.

In addition to the previous tests, a simulation test is carried out to examine the PCM’s response to an overload situation and to verify that the 5V line stays within the specified parameters. The results of this test, including all possible cases and the minimum and maximum voltage, are presented in Fig. 23.

The integration of the PCM has enabled the removal of the need for a separate 5V external power supply. The CAN bus is now powered directly from the PCM. It is important to verify that telemetry data is received on both nodes of the CAN network. Additionally, the power consumption of the system should be measured, as outlined in Fig. 24. This will provide valuable insights into the performance of the PCM and the overall efficiency of the system.

4.2 Power distribution unit

The PDM serves an important role in power distribution from both the PCM and battery to the sub-systems. It provides crucial circuit protection by using a combination of resettable circuit breakers and fused lines to ensure the safe and reliable supply of power to the receivers and power system.

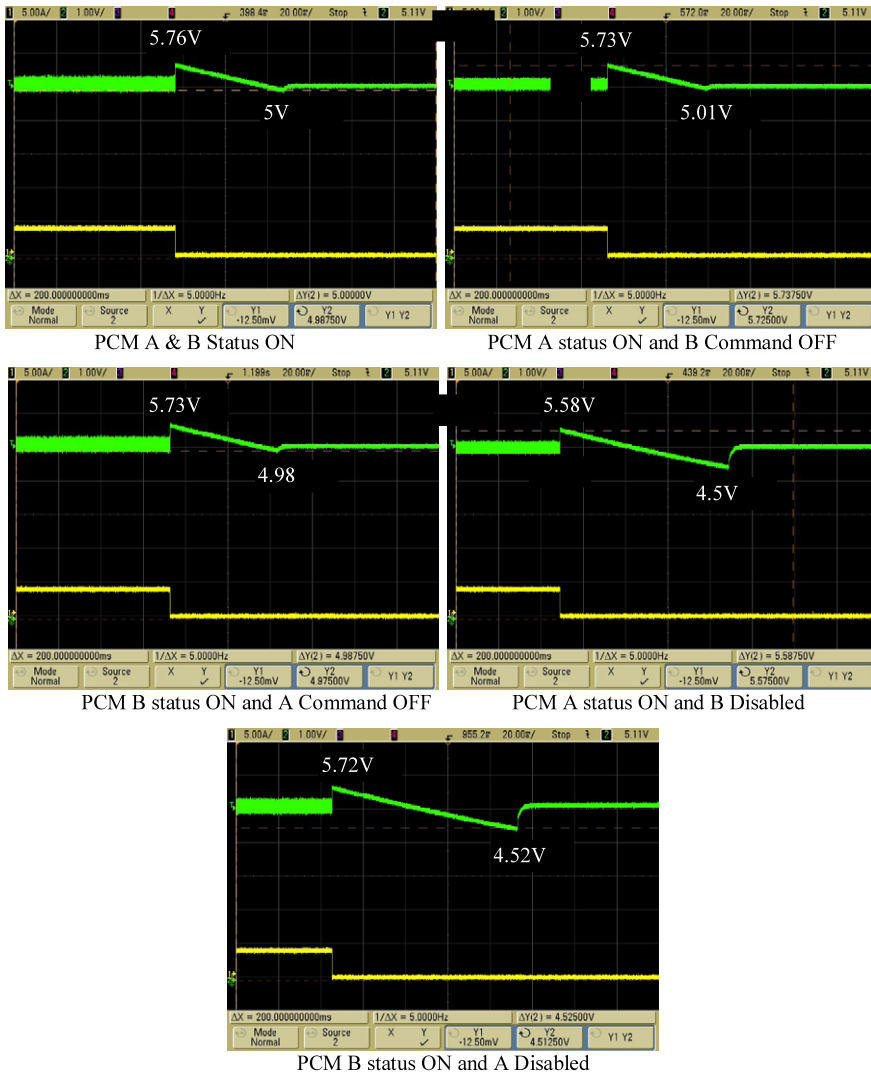


Figure 23. PCM overload.

4.2.1 TCL switches

The TCL switches require two key measurements to be made to ensure their proper function: the inrush capability of the switch and the trip current level. To assess the inrush capability, a capacitive load response test is conducted to ensure the switch can provide the expected inrush current at switch-on. The switch should remain on, and the current drawn should decrease to zero once the capacitor has fully charged. During the tests, the voltage across the capacitor and the current from the switch to the capacitor are recorded and captured in the oscilloscope waveforms shown in Fig. 25. This test is repeated for all TCL switches.

To properly evaluate the TCL switches, two measurements must be made: the inrush capability and the trip current level. The capacitive load response of the switch is tested to verify its ability to provide the expected current inrush during switch-on. The switch should remain on until the capacitor is fully charged and the current drawn should drop to zero. The test results, including the oscilloscope waveforms of voltage across the capacitor and current from the switch to the capacitor, are depicted in Fig. 25 and are repeated for all TCL switches. It's important to note that a resistive load should never

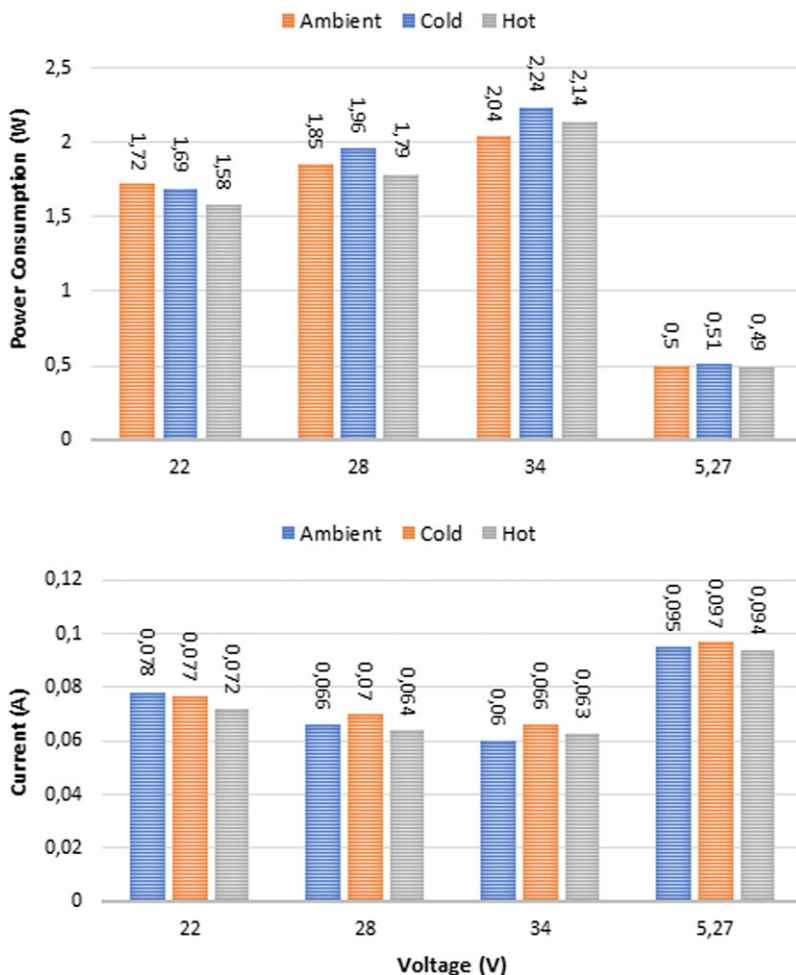


Figure 24. Telemetry check on CAN nodes.

be used to test the trip setting on TCL switches. The oscilloscope waveforms of voltage across the trip resistor and current from the switch to the trip resistor are recorded and shown in Fig. 26 for all TCL switches.

Flow in response to overloading conditions, whether caused by resistive loads such as heating elements or by capacitive loads, such as motors and power supplies. This ability to handle a diverse range of loads is a key feature of TCL switches, ensuring reliable and safe performance in a variety of applications (see Fig. 27).

4.2.2 FCL switches

The input voltage for the test is set to a minimum of 24V, with the current limit set to 20% above the switch’s trip setting. The test is also performed with a maximum input voltage of 34V. If the current ever surpasses the trip level, the TCL switch will initiate current limiting to protect against overloading. During this process, if the output voltage drops, the current limit will automatically adjust to a lower level, minimising dissipation in the FET. The recorded trip current results are depicted in Fig. 28, providing a clear representation of the switch’s performance.

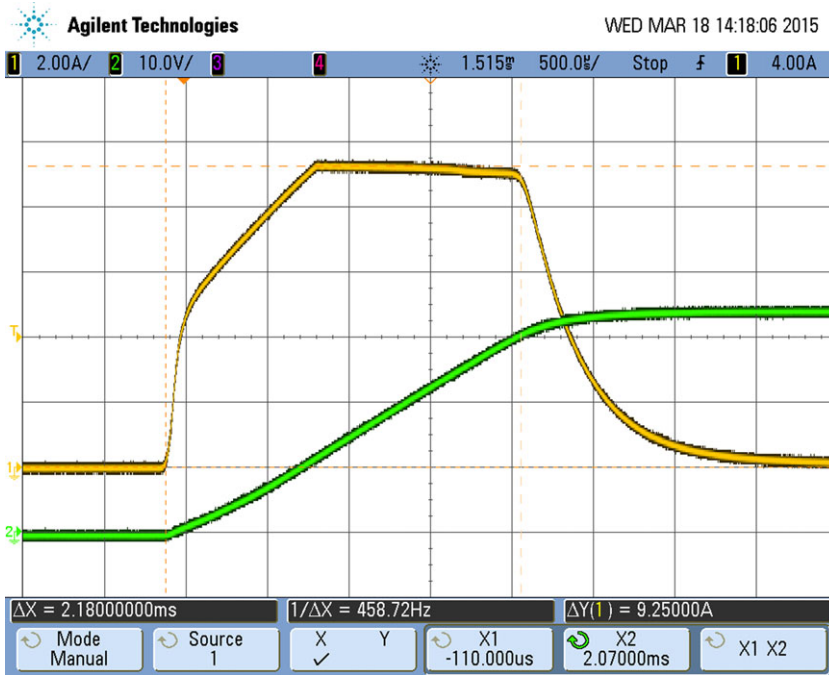


Figure 25. TCL switch capacitive load response waveform.



Figure 26. TCL switch resistive load response waveform: (a) ambient, (b) cold and (c) hot temperature.

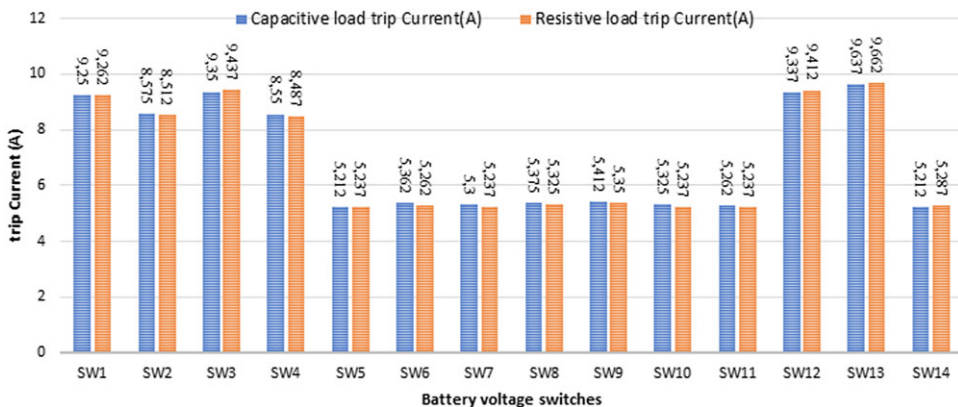


Figure 27. TCL switch capacitive and resistive load trip current.

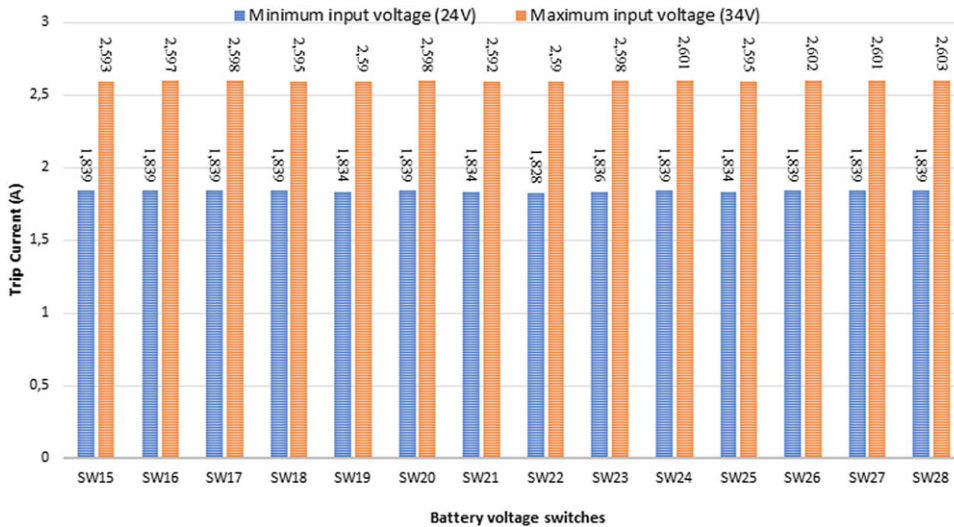


Figure 28. FCL switch trip current.

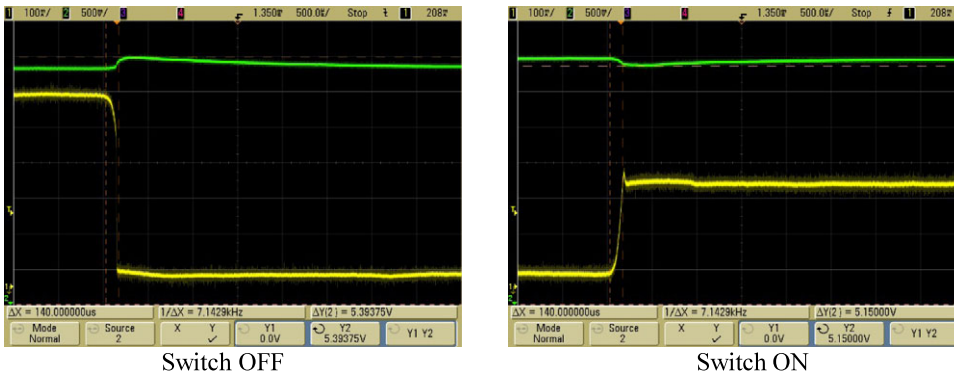


Figure 29. 5V FET switch waveform.

4.2.3 5V FET switches

The test procedure included capturing waveforms to demonstrate the stability of the 5V line for the four switches used (SW4, SW5, SW7 and SW9). The waveform of switch four (SW4) is shown in Fig. 29. It is crucial that both PCMs are kept in the on state throughout the test, as this will provide accurate and meaningful results. The waveform recordings provide valuable information about the stability of the 5V line and the performance of each switch, allowing for a thorough analysis and assessment of the system’s capabilities.

The waveforms of the 5V FET switches were analysed to determine the maximum and minimum voltage levels of the PCMs at the point when the switch trips to the off state. This data is depicted in Fig. 30, providing a clear visual representation of the voltage levels during the tripping process. By recording the PCM voltages during switch tripping, it is possible to gain valuable insights into the stability and performance of the system, and identify any potential areas for improvement.

To enhance the understanding of the PCM-PDM module’s functionality, we’ve incorporated a Fig. 31 showcasing its interaction with other subsystems through various switches. Additionally, this figure

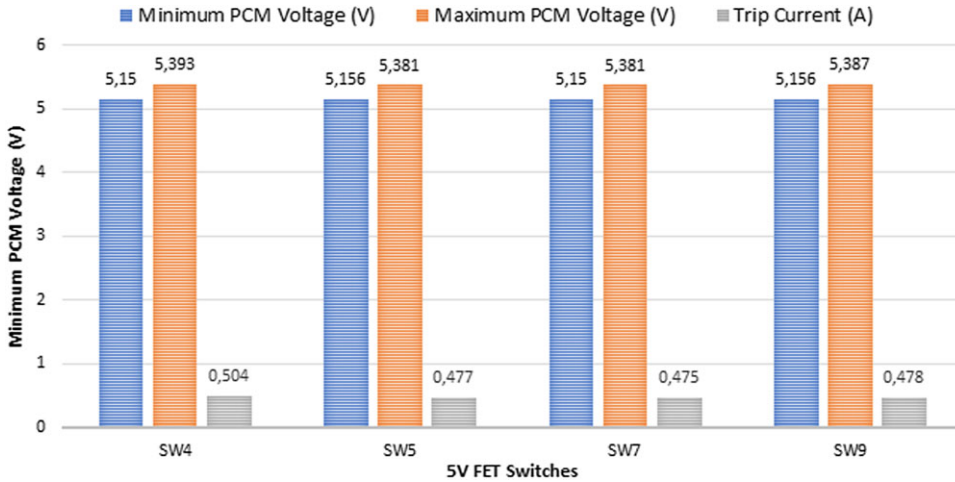


Figure 30. 5V FET switches minimum/maximum voltage and trip current.

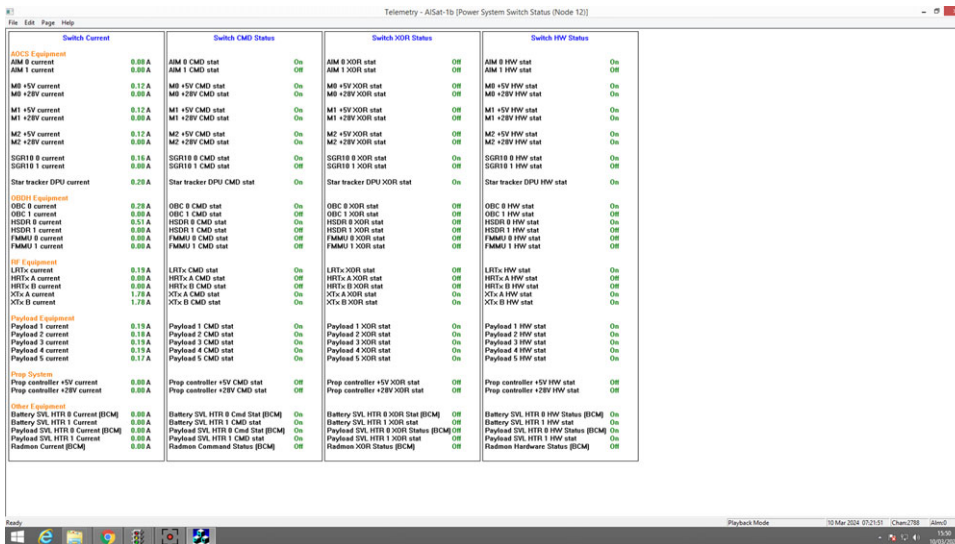


Figure 31. PCM-PDM switches state in nominal mode.

displays the last telemetry (TLM) data collected during the module’s operation in space, providing valuable insights into its performance in real-world conditions.

During nominal mode, when no imaging or transmission operations occur, most subsystems are deactivated (see Fig. 31), with switches set to the off state. However, essential subsystems, such as the on-board computer (OBC) and reaction wheels, remain activated to ensure the satellite’s basic functionality.

During imaging-downlink mode, the majority of subsystems are activated by toggling the dedicated switches of the PCM-PDM module to the on state, ensuring precise satellite pointing and stability throughout the operation. Figure 32 visually demonstrates the activation of all attitude and orbit control system (AOCS), payload and X band transmitter (xTx) equipments. Given the substantial power consumption involved, the battery discharge is warranted to support this operation.

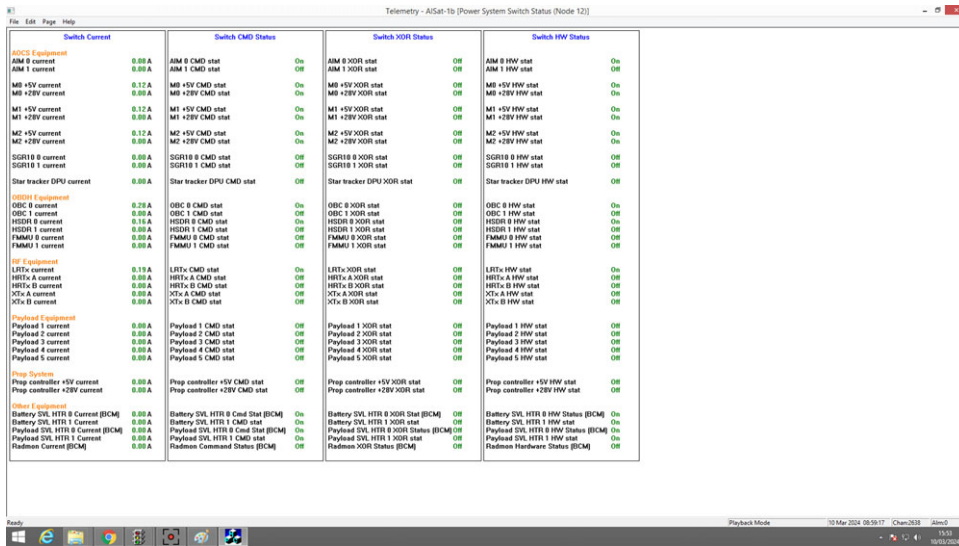


Figure 32. PCM-PDM switches state in imaging-downlink mode.

5.0 Conclusion

On the completion of testing the PCM-PDM, this paper summarises the results of the tests, including waveforms, and describes the performance of the module during the tests.

In conclusion, the design, manufacture, performance testing and integration of a PCM-PDM on the Alsat-1B satellite is a critical component of the satellite system. The PCM-PDM is responsible for converting, regulating and distributing power to various subsystems and payloads in space, and its design must consider factors such as power conversion efficiency, power conditioning, voltage and current regulation, thermal management and fault protection. The manufacturing process must be rigorous to ensure the high reliability and robustness of the components and the overall system, given the harsh conditions it will be exposed to in space. The performance testing validate the functionality and efficiency of the PCM-PDM, including its ability to withstand radiation, extreme temperatures and other environmental factors. The successful integration of the PCM-PDM into the Alsat-1B satellite system is essential for the reliable operation and achievement of the satellite’s mission objectives.

The integration of the PCM-PDM into the Alsat-1B satellite system was a resounding success, resulting in a reliable and efficient operation that has helped ensure the achievement of the satellite’s mission objectives. This accomplishment has been reflected in the outstanding performance of the module in orbit since the Alsat-1B satellite was launched. To date, the PCM-PDM has demonstrated optimum operation, making a significant contribution to the overall success of the satellite mission.

References

- [1] Bettencourt J.C. and Stengel R.B. Power conditioning and switching for small satellites. Published in the *J. Aerosp. Eng.*, 2021, **3**, pp 36–52.
- [2] King R.W.P. and Beach G.W. An overview of power switching and conditioning circuits for small satellites. Published in the *J. Aerosp. Eng.*, 2021, **3**, pp 41–56.
- [3] Patel M.R. and Beik O. *Spacecraft Power Systems*, 2nd ed., CRC Press, 2023. ISBN: 9781003804215.
- [4] Shen P.X., Fang J.Y. and Zhang T.X. Power switching and conditioning circuit design for microsattellites. Published in the *J. Aerosp. Eng.*, 2018, **2**, pp 21–38.
- [5] Williams T. *The Circuit Designers Companion*, 2nd ed.: Newnes, 2004. ISBN: 9780080476513.
- [6] Bensaada M., Mebrek M.A. and Schofield D. Power system design and performance for low earth orbit spacecraft. *IEEE Aerosp. Electron. Syst. Mag.*, 2022, **37**, (1), pp 44–58. doi: [10.1109/MAES.2021.3117356](https://doi.org/10.1109/MAES.2021.3117356)
- [7] Bekhti M., Bensaada M. and Beldjehem M. Design and implementation of a power distribution system adopting overcurrent protection. *Aeronaut. J.*, 2020, **124**, (1281). ISSN: 0001-9240.

- [8] Alsat-1b Battery Charge Module Interface Control Document: SSTL, 2014.
- [9] Rodriguez J., Gonzalez R. and San Martin E. Flyback converter design for high-density power supplies. *IEEE Trans. Power Electron.*, 2010, **25**, (4), pp 969–978.
- [10] Rodriguez J., Gonzalez R. and San Martin E. High-efficiency Flyback converters for portable applications. *IEEE J. Emerg. Sel. Top. Power Electron.*, 2015, **3**, (4), pp 754–764.
- [11] Rodriguez J. and Gonzalez R. Flyback converter design for low-power applications. *IEEE J. Emerg. Sel. Top. Power Electron.*, 2016, **4**, (2), pp 593–604.
- [12] Lee J.W., A compact current-controlled foldback power limiter with enhanced load-current monitoring capability. *IEEE Trans. Circuits Syst. II Express Briefs*, 2021, **68**, (5), pp 489–493.
- [13] Tan T.K. A high-efficiency current-mode foldback regulator with output current limiting. *IEEE Trans. Power Electron.*, 2019, **34**, (4), pp 3636–3645.
- [14] Kim S.H. and Kim Y.W. Design of foldback current limiter with output current monitoring circuit. *J. Electromagn. Eng. Sci.*, 2018, **18**, (1), pp 47–53.
- [15] Chen Y.Q., Zhang Y.X. and Liu Z.Q. Design and analysis of foldback current limiter based on adaptive hysteresis control. *J. Electromagn. Waves Appl.*, 2016, **30**, (9), pp 1075–1086.
- [16] Bhatia M.K., Chugh K.K. and Grewal S.S. A high efficiency foldback current limiter for dc-dc converters. *J. Power Electron.*, 2015, **15**, (5), pp 962–970.
- [17] Lee J.K. A novel Timed Current Latch (TCL) regulator with foldback current limiting. *IEEE J. Solid-State Circuits*, 2003, **38**, (2), pp 242–250.
- [18] Liu X. and Su H.J. A simple and high-efficiency timed current latch power supply with foldback current limiter. *J. Power Electron.*, 2006, **6**, (4), pp 392–401.
- [19] Wang L.X. and Liu Y.X. A novel timed current latch regulator with adaptive on-time control. *J. Electromagn. Waves Appl.*, 2008, **22**, (14), pp 1915–1924.
- [20] Du J.L. and Yin X.Y. A timed current latch regulator with dual mode control for switching power supplies. *J. Electromagn. Waves Appl.*, 2011, **25**, (7–8), pp 1037–1046.
- [21] Joffe E.B. and Lock K.-S. *Grounds for Grounding: A Circuit-to-System Handbook*. 1st ed., IEEE, 2010. ISBN 978-0471-66008-8.
- [22] Electrical grounding architecture for unmanned spacecraft, NASA TECHNICAL HANDBOOK, NASA-HDBK-4001, February 17, 1998.
- [23] Boncyk W.C. Developing a distributed power and grounding architecture for PnPSat. 2008 IEEE Aerospace Conference, 01-08 March 2008, IEEE, Big Sky, MT, USA. doi:[10.1109/AERO.2008.4526506](https://doi.org/10.1109/AERO.2008.4526506).
- [24] Liu Y.A. and Liu Y.Y. *Grounding and Isolation in Spacecraft Electric Power Systems*: Publisher Springer, Vol. 4, 2015, pp 15–28.